

A Venus in the Making? Predictions for *JWST* Observations of the Ultracool M-Dwarf Planet LP 890-9 c

Jonathan Gomez Barrientos ^{1,2*}, Lisa Kaltenegger ¹, and Ryan J. MacDonald ^{1,3,4}

¹Carl Sagan Institute and Department of Astronomy, Cornell University, Ithaca, NY 14853, USA

²Division of Geological and Planetary Sciences, California Institute of Technology, Pasadena, CA 91125, USA

³Department of Astronomy, University of Michigan, Ann Arbor, MI 48109, USA

⁴NHFP Sagan Fellow

Accepted 2023 May 10. Received 2023 April 25; in original form 2022 December 23

ABSTRACT

The recently discovered transiting super-Earth LP 890-9 c is potentially one of the best rocky exoplanets for atmospheric characterization. Orbiting an ultracool M-dwarf at the inner edge of the habitable zone, LP 890-9 c offers a new opportunity to study the climate of rocky planets at the inner edge of the habitable zone. We investigate the molecular detectability with simulated *JWST* transmission spectra for five potential atmospheres of LP 890-9 c. We find that a small three-transit *JWST* program can infer evidence of H₂O (at 3 σ confidence) for a full runaway greenhouse scenario. Alternatively, CO₂-dominated atmospheres resembling Venus without high-altitude terminator clouds can be identified with eight transits. However, these predictions could be complicated by the impact of clouds and/or unocculted starspots. Nevertheless, *JWST* observations of LP 890-9 c could provide critical insights and potentially distinguish between models of rocky planets at the inner edge of the habitable zone.

Key words: planets and satellites: terrestrial planets – planets and satellites: individual (LP 890-9 c) – planets and satellites: atmospheres – techniques: spectroscopic

1 INTRODUCTION

Planets orbiting ultra-cool M dwarf stars present one of the best opportunities to characterize terrestrial exoplanet atmospheres. The best known example, the TRAPPIST-1 system (Gillon et al. 2016, 2017), has ignited intense theoretical and observational study since its discovery in 2016. With *JWST* fully operational, the atmospheres of these rare ultra-cool M dwarf planets can now be explored.

Recently, Delrez et al. (2022) reported the discovery of two transiting super-Earths around the low-activity M6 dwarf LP 890-9 (also known as TOI-4306 or SPECULOOS-2). The second planet in the system, LP 890-9 c — discovered by the ground-based SPECULOOS survey (Gillon 2018; Sebastian et al. 2021) — has a radius of $1.367^{+0.055}_{-0.039} R_{\oplus}$, an orbital period of 8.46 days, and receives slightly less irradiation than Earth ($0.906 \pm 0.026 S_{\oplus}$). Since M dwarfs warm Earth-like planets more effectively than Sun-like stars (see, e.g., Kasting et al. 1993), LP 890-9 c lies very close to the inner edge of the conservative habitable zone (HZ) (Kopparapu et al. 2013, 2017). After the TRAPPIST-

1 planets, LP 890-9 c is the next best HZ terrestrial planet for atmospheric characterization with *JWST* (Delrez et al. 2022), while also providing initial insights into the conditions of a potentially habitable world at the inner edge of the conservative HZ.

Recently, Kaltenegger et al. (2022) presented initial atmospheric models for five possible atmospheres of LP 890-9 c: (1) a Hot Earth analogue; (2) a moist greenhouse with the same CO₂ abundance as the modern Earth; (3) a moist Runaway Greenhouse with 20% of the CO₂ abundance of the dry atmosphere; (4) a Full Runaway Greenhouse with a steam atmosphere; and (5) a modern Venus analogue dominated by CO₂. In what follows, we refer to these five models as ‘Hot Earth’, ‘Runaway 1,2,3’, and ‘Exo-Venus, cloud-free’. The Hot Earth scenarios uses modern Earth models at the orbital distance of LP890-9c. Runaway 1 and 2 show increasing surface temperature (T_{surf}) and increasing water vapor in the atmosphere, which in turn increases the total surface pressure (P_{surf}) as expected for terrestrial planet atmospheres near the inner edge of the HZ, leading to a P_{surf} of 1.27 bar and 3.86 bar for these scenarios. Runaway 3 shows a full runaway greenhouse steam atmosphere, with a P_{surf} of 271 bar, and T_{surf} of 1600 K. The Exo-Venus scenario uses

* E-mail: jgomezba@caltech.edu

the CO₂ dominated atmospheric model with P_{surf} of 153 bar and T_{surf} of 599 K. All five models assume no clouds at the terminator region. To explore the effect of Venus-like clouds, we also consider an opaque cloud layer at 70km for the Exo-Venus scenario.

In this Letter, we evaluate the ability of *JWST* to characterize the atmosphere of LP 890-9 c. Since planets at the inner edge of the conservative HZ like LP 890-9 c can sustain several very different possible atmospheres (see e.g., [Faucher et al. 2022](#); [Turbet et al. 2020](#); [Kaltenegger et al. 2022](#)), depending on the initial water inventory and the water loss timescales, we consider the five scenarios described above. We perform an atmospheric retrieval analysis for these possible atmospheres of LP 890-9 c, which could represent steps in the evolution of a terrestrial planet from an Earth-like planet to one resembling Venus ([Kaltenegger et al. 2022](#)). Our retrieval analysis quantifies the molecular detectability and anticipated abundance constraints for each LP 890-9 c atmospheric scenario, demonstrating the priority of observing this tantalizing planet with *JWST*.

2 METHODS

2.1 Model Spectra of LP 890-9 c

We model and retrieve transmission spectra for five atmospheres for LP 890-9 c ([Kaltenegger et al. 2022](#)) with the radiative transfer and retrieval code POSEIDON ([MacDonald & Madhusudhan 2017](#); [MacDonald 2023](#)). First, we use POSEIDON’s forward model, TRIDENT ([MacDonald & Lewis 2022](#)), to compute transmission spectra from the 1D atmospheric pressure-temperature (P-T) and chemical abundance profiles from [Kaltenegger et al. \(2022\)](#). We interpolated these profiles onto a 100-layer vertical grid evenly spaced in log-pressure from 10^{-7} –10 bar. We assign the planet’s white light radius ($1.37 R_{\oplus}$) to the surface and compute a new reference radius at a pressure of 1 mbar and, in lieu of a mass measurement, adopt the predicted median mass of $2.5 M_{\oplus}$ ([Delrez et al. 2022](#)) from a mass-radius relationship ([Chen & Kipping 2017](#)). For the radiative transfer calculation, our models consider N₂, H₂O and CO₂ (following [Kopparapu et al. 2013](#)), with the exception of the Hot Earth scenario that additionally includes O₂, O₃, CH₄ and N₂O. The opacity data used by TRIDENT are described in [MacDonald & Lewis \(2022\)](#) (their Appendix C).

Since the anticipated cloud pressure level for LP 890-9 c is uncertain, in this initial study we generally solve for the radiative transfer assuming clear atmospheres. However, we briefly explore the effect of clouds by adding an opaque surface, concealing layers deeper than 70 km altitude, to the Exo-Venus model. Our model transmission spectra are shown in Figure 1.

2.2 Simulated *JWST* Observations

To assess the number of transits of LP 890-9 c required to detect key molecular species, we next generated simulated *JWST* data using PandExo ([Batalha et al. 2017](#)). We considered 1 to 200 transits to generate synthetic *JWST* observations, depending on the atmospheric scenario, to investigate how many transits are required to achieve at least a

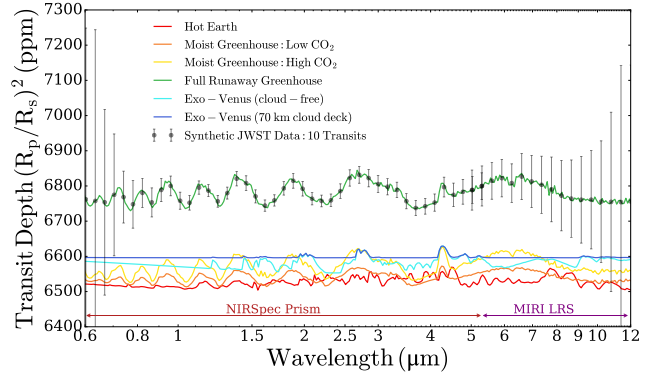


Figure 1. Model transmission spectra and simulated *JWST* observations of LP 890-9 c. The atmospheric scenarios from [Kaltenegger et al. \(2022\)](#) (colored lines) are shown binned to a spectral resolution of $R = 100$. We overplot *JWST* NIRSpec PRISM and MIRI LRS simulations, assuming 10 transits with each mode, without Gaussian scatter, and binned to $R = 20$, for the Full Runaway Greenhouse model (Runaway 3) (the error bars have the same magnitude for the other scenarios). The transit depth offset between the Runaway 3 model and the other scenarios arises from the extended H₂O-rich atmosphere (substantially increasing the 1 mbar planet radius).

3 sigma detection for a given molecule. We initially considered both NIRSpec PRISM (0.6–5.3 μm) and MIRI LRS (5–12 μm) observations to explore the full wavelength coverage of our model transmission spectra. For NIRSpec PRISM, we use the 512 subarray. For both instruments, we limit the saturation to 80% full well. We keep all simulated observations at their native resolution for retrieval purposes to avoid losing information by binning to a specific spectral resolution. We use the stellar spectrum from [Delrez et al. \(2022\)](#), normalized to a magnitude of $J = 12.258$. Finally, we assume an observation baseline for each transit of three times the transit duration (3×57.56 min; [Delrez et al. 2022](#)).

Figure 1 shows our simulated *JWST* observations for 10 transits with NIRSpec PRISM and 10 transits with MIRI LRS. Given the large error bars of the MIRI observations, and noting that previous retrieval studies have found that NIRSpec PRISM has the greatest information content (e.g. [Batalha et al. 2019](#); [Lin et al. 2021](#)), we only include the NIRSpec PRISM observations in our subsequent retrievals. For our retrieval analysis, we omit Gaussian scatter from the synthetic data and instead center the data on its (true) binned model location — this essentially produces a mean retrieval result unaffected by a specific random noise draw (see [Feng et al. 2018](#)).

2.3 Atmospheric Retrieval Analysis

We use the atmospheric retrieval code POSEIDON ([MacDonald & Madhusudhan 2017](#)), which couples a parametric form of the transmission spectrum model described above with the nested sampling algorithm PyMultiNest ([Feroz et al. 2009](#); [Buchner et al. 2014](#)), to establish predicted constraints on LP 890-9 c’s atmosphere. We divide the atmosphere of LP 890-9 c into 100 layers equally spaced in log-pressure from 10^{-7} –10 bar. We parameterize the P-T profile as a free gradient (linear in log-pressure) between

10^{-5} and 1 bar (MacDonald & Lewis 2022), described by the temperatures at these boundary pressures (each with a uniform prior from 100–800 K). Two parameters are assigned for the 1 mbar reference radius of the planet (uniform prior from $0.8\text{--}1.2 R_p$) and for the surface/cloud pressure (log-uniform prior from $10^{-7}\text{--}10$ bar). Since the molecule dominating LP 890-9 c's atmosphere is *a priori* unknown, and differs across our five atmosphere scenarios, we adopt the centered log-ratio (CLR) of the gases as free parameters (e.g. Aitchison 1986; Benneke & Seager 2012). The CLR parameterization treats all gases with equal priors, while automatically accounting for the summation to unity constraint of mixing ratios (Benneke & Seager 2012). For the Runaway Greenhouse and Exo-Venus models, we fit for the CLR-transformed mixing ratios of H_2 , H_2O , and CO_2 . For the Hot Earth scenario, we fit six parameters for O_2 , O_3 , H_2O , CO_2 , CH_4 , and N_2O . The CLR priors span the parameter space from a minimum mixing ratio of 10^{-12} to any of the gases dominating the atmosphere (see Lustig-Yaeger & Fu et al. 2023). We fill the remaining atmosphere with N_2 (specified by the summation to unity condition without requiring a free parameter). Thus, depending on the atmospheric scenario, our retrievals contain a total of 7–10 free parameters. All our retrievals sample the parameter space with 2000 MultiNest live points.

We conducted a total of 54 retrievals. For each simulated dataset, we perform a retrieval with the full reference set of parameters described above. We then computed additional nested retrievals with a single gas removed. By comparing the Bayesian evidences of these models, we compute predicted detection significances of H_2O , CO_2 , CH_4 , and N_2O as a function of the number of transits through Bayesian model comparisons (see e.g., Benneke & Seager 2013; Trotta 2017).

3 RESULTS: JWST PREDICTIONS FOR LP 890-9 C

Our transmission spectra show marked differences between the model atmospheres (Figure 1, see also Kaltenecker et al. 2022). Hence, we find that even moderately sized JWST programs can distinguish between different atmospheric scenarios that are crucial for understanding the nature of planets near the inner edge of the HZ. Figure 2 demonstrates this for two such scenarios: a H_2O -dominated Full Runaway Greenhouse (Runaway 3), a CO_2 -dominated cloud-free Exo-Venus. In each case, our retrievals demonstrate that < 10 transits with JWST could establish whether LP 890-9 c's atmosphere is dominated by H_2O or CO_2 . The third case shown in Figure 2 shows that 20 JWST transits could identify N_2O in the atmosphere of a Hot Earth scenario, which could provide a stable habitable environment for LP 890-9 c (Kaltenecker et al. 2022).

Figure 3 shows our predicted molecular detection significances for LP 890-9 c. The most readily detectable atmosphere arises from the Full Runaway Greenhouse scenario (Runaway 3), for which the extended H_2O atmosphere produces strong H_2O absorption features (see Figure 2). In this Runaway 3 state, one could detect H_2O to $> 3\sigma$ confidence in as few as three NIRSpec PRISM transits. Our moist greenhouse scenarios require additional transits to detect

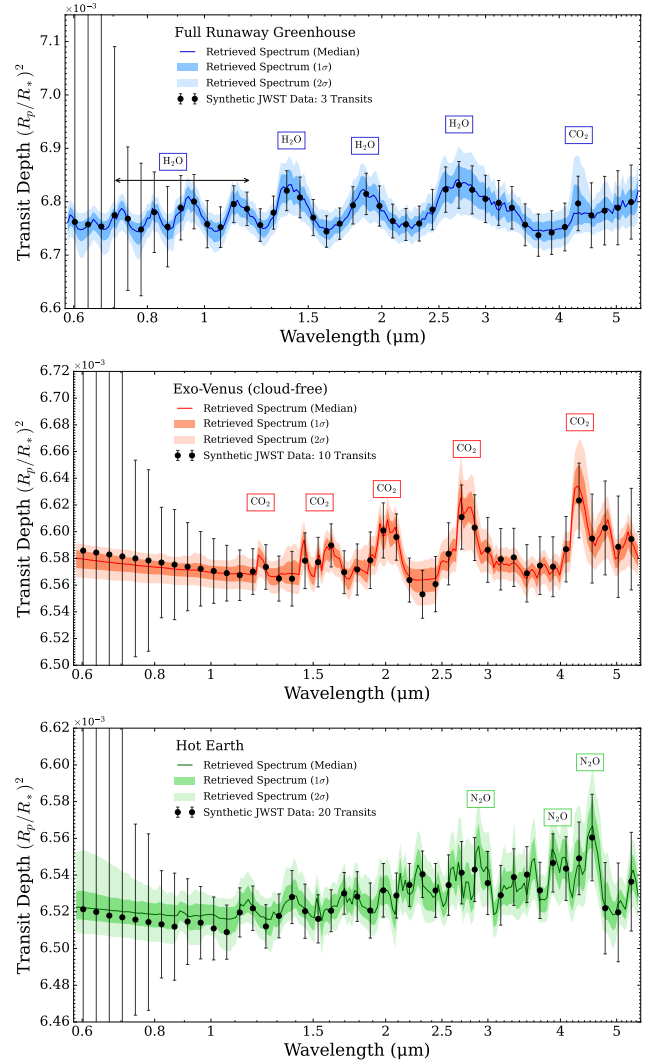


Figure 2. Retrieved transmission spectra from simulated JWST observations of LP 890-9 c. *Top:* Three synthetic NIRSpec PRISM observations of the 5 bar Full Runaway Greenhouse scenario (Runaway 3). *Middle:* Ten synthetic NIRSpec PRISM observations of the 5 bar cloud-free Exo-Venus scenario. *Bottom:* Twenty synthetic NIRSPEC PRISM observations of the 1 bar Hot Earth scenario. The median retrieved transmission spectra (solid line) and the $1\sigma/2\sigma$ (shaded regions) are shown. The most prominent spectral features are labeled. All datasets are shown binned to a spectral resolution of $R=20$ for clarity and without Gaussian scatter.

H_2O to $> 3\sigma$: 4 transits for Runaway 2 with 20% CO_2 abundance and 11 transits for Runaway 1 with the Earth-analog CO_2 abundance ($\sim 10^{-4}$). This arises from a combination of their lower atmospheric H_2O abundance and/or the smaller scale height from their higher CO_2 abundance compared to the Full Runaway Greenhouse (Runaway 3). One can also detect CO_2 itself to $> 3\sigma$ with 20 transits for the Runaway 2 scenario. Our cloud-free baseline Exo-Venus model, however, requires just 8 transits for a 3σ CO_2 detection. CO_2 is the most readily detectable molecule for the cloudless Exo-Venus scenario (see Figure 2) due to both its prominent near-infrared absorption features (e.g. The JWST Transit-

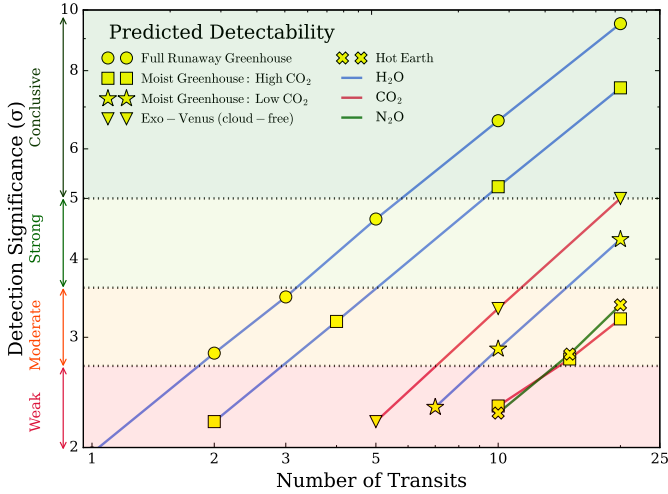


Figure 3. Predicted molecular detection significances for five possible LP 890-9 c atmosphere models as a function of *JWST* NIRSpec PRISM transits. The detection significances are categorized as ‘weak’, ‘moderate’, ‘strong’, and ‘conclusive’ detections (colored regions), according to an adaptation of the Jeffreys’ scale for Bayesian model comparisons (Trotta 2017). The boundaries (dotted lines) between the different categories occur at 2.7σ , 3.6σ , and 5.0σ . The marker symbols correspond to each atmospheric scenario, while the line colors corresponds to each molecule.

ing Exoplanet Community Early Release Science Team et al. 2022) and its uniquely high mean molecular weight — the latter allowing the CLR retrieval parameters to identify CO_2 as the bulk atmospheric consistent. However, should LP 890-9 c have a cloud coverage resembling the modern Venus, we find that 65 transits would be required to achieve the same 3σ CO_2 detection. Finally, the most observationally challenging scenario corresponds to LP 890-9 c being in a potentially stable habitable stage, before evolving into a Venus-like planet (our ‘Hot Earth’ scenario). For the Hot Earth scenario, 20 transits would be required to detect N_2O to $> 3\sigma$. The second most detectable species in this scenario is CH_4 , but with at least 40 transits for a 3σ detection. All other species (O_2 , O_3 , H_2O , and CO_2) in the Hot Earth model require > 100 transits to be detected.

Figure 4 shows our predicted abundance constraints for H_2O , CO_2 , N_2O , and CH_4 for 5, 10 and 20 NIRSpec PRISM transits. Our results indicate that 5 transits with *JWST* could suffice to identify whether the main atmospheric component is H_2O or CO_2 (consistent with Batalha et al. 2018), as illustrated by the cloud-free Exo-Venus and Full Runaway Greenhouse (Runaway 3) posteriors in Figure 4. Across all three runaway greenhouse models, only lower limits can be placed on the H_2O abundance. With 10 transits, we predict 2σ H_2O abundance constraints of: $> 0.003\%$ (Runaway 1), $> 0.5\%$ (Runaway 2), and $> 3\%$ (Runaway 3). We find that the best prospect for distinguishing our atmospheric scenarios arises from the retrieved CO_2 abundances. With 20 transits, our cloud-free Exo-Venus scenario has a strong lower limit on the CO_2 abundance ($> 59\%$ to 2σ) while the three Runaway Greenhouse models have substantially lower retrieved CO_2 abundances. Runaway 2 is especially promising, with a bounded constraint on the CO_2 abundance ($\log \text{CO}_2 = -1.53^{+0.81}_{-1.65}$). Finally, our Hot Earth scenario is the most

challenging to characterize due to its small spectral features (see Figure 1). With 20 transits of the Hot Earth, we find a lower limit on the N_2O abundance (corresponding to the 3σ N_2O detection in Figure 3) and a hint of CH_4 . We provide a full table containing our predicted abundance constraints in the supplementary material.

4 SUMMARY AND DISCUSSION

The recently discovered super-Earth LP 890-9 c presents a rare opportunity to shed light on how the climates of rocky planets evolve at the inner edge of the habitable zone. We explored *JWST*’s ability to characterize LP 890-9 c’s atmosphere given a series of possible atmosphere scenarios. We find that the feasibility of characterizing the atmosphere strongly depends on the atmospheric scenario, with the most promising scenario being a Full Runaway Greenhouse scenario for which H_2O could be detected to 3σ with a small 3-transit *JWST* NIRSpec PRISM program. A more ambitious 8-transit program could detect CO_2 for a Venus-like atmosphere without high-altitude clouds at the terminator, allowing H_2O -rich and CO_2 -rich scenarios to be distinguished. Finally, a 20-transit program could even reveal N_2O signatures for a potentially habitable Hot Earth scenario. Observations with *JWST* can therefore provide critical insights into the planetary environment. Our results suggest that, if LP 890-9 c is in the process of becoming an Exo-Venus, *JWST* may be able to differentiate between our modeled evolutionary stages through which specific molecules are detected (see Figures 2 and 3).

Finally, we note that some of the key assumptions in this work will benefit from further exploration in future studies. In particular, we have not fully investigated the impact of clouds or unocculted starspots on our retrieval results. Recent 3D general climate models (GCM) have demonstrated that clouds should concentrate on the night side for tidally locked rocky planets with the insolation of early Venus or early Earth (Turbet et al. 2021). Therefore, clouds may not influence transmission spectra for planets like LP 890-9 c if they do not extend to the terminator region. However, further assessing the impact of clouds will require future 3D GCM models for this planet with varying cloud assumptions. Our non-inclusion of contamination from unocculted starspots (i.e. the transit light source effect; Rackham et al. 2018) is motivated by the low-activity of LP 890-9 (Delrez et al. 2022), which could simplify analyses of LP 890-9 c’s transmission spectrum compared to the TRAPPIST-1 planets (e.g. Zhang et al. 2018; Wakeford et al. 2019). However, future observations and further studies will be required to assess the relative importance of the transit light source effect for the LP 890-9 system.

Ultimately, observations of LP 890-9 c can serve to directly test both GCM predictions (by determining whether the transmission spectrum is feature-rich or featureless) and to search for signatures of stellar contamination (via short wavelength slopes). In either case, *JWST* observations of LP 890-9 c have the potential to provide critical new insights into our understanding of warm rocky planets that reside near the inner HZ of ultracool M-dwarfs.

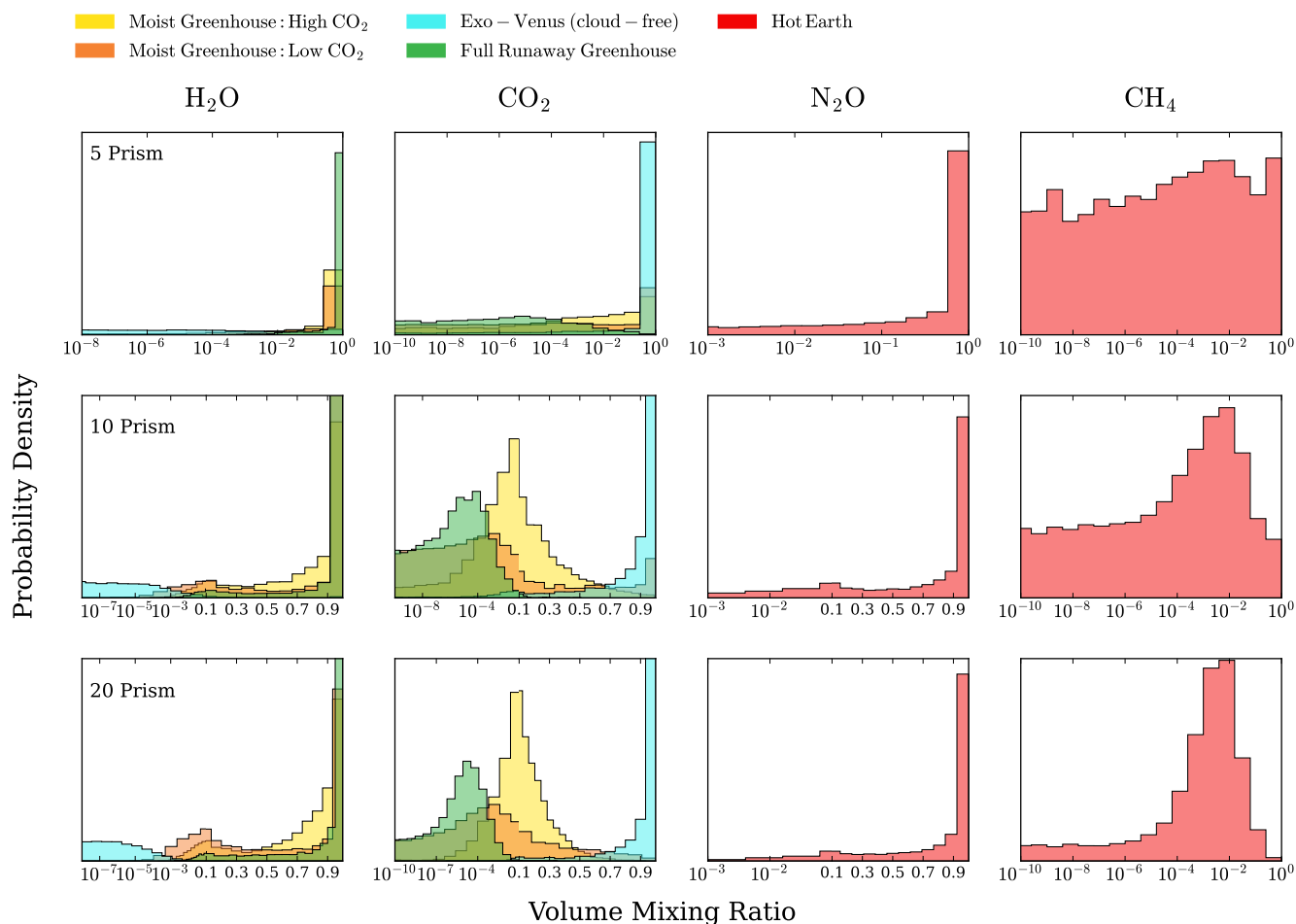


Figure 4. Predicted molecular abundance constraints for five potential atmospheres of LP 890-9 c. The posterior probability distributions of the molecular abundances are shown for 5, 10, and 20 *JWST* NIRSPEC PRISM transits (top, middle, and bottom, respectively). For ease of viewing, we omit the unconstrained H₂O and CO₂ posteriors for the Hot Earth. We note that only the Hot Earth scenario contains N₂O and CH₄ in the atmospheric model.

ACKNOWLEDGEMENTS

We thank the anonymous referee for a helpful report. JGB is supported by the Rose Hills Foundation. LK and JGB acknowledge support from the Brinson Foundation "Search for Life" and the Carl Sagan Institute. RJM acknowledges that support for this work was provided by NASA through the NASA Hubble Fellowship grant HST-HF2-51513.001 awarded by the Space Telescope Science Institute, which is operated by the Association of Universities for Research in Astronomy, Inc., for NASA, under contract NAS5-26555.

DATA AVAILABILITY

Additional figures are available in the supplementary online material <https://doi.org/10.5281/zenodo.7922765>.

REFERENCES

Aitchison J., 1986, *The Statistical Analysis of Compositional Data*. Monographs on Statistics and Applied Probability,

- Springer Netherlands
 Batalha N. E., et al., 2017, *PASP*, **129**, 064501
 Batalha N. E., Lewis N. K., Line M. R., Valenti J., Stevenson K., 2018, *ApJ*, **856**, L34
 Batalha N. E., Marley M. S., Lewis N. K., Fortney J. J., 2019, *ApJ*, **878**, 70
 Benneke B., Seager S., 2012, *ApJ*, **753**, 100
 Benneke B., Seager S., 2013, *ApJ*, **778**, 153
 Buchner J., et al., 2014, *A&A*, **564**, A125
 Chen J., Kipping D., 2017, *ApJ*, **834**, 17
 Delrez L., et al., 2022, *A&A*, **667**, A59
 Fauchez T. J., et al., 2022, *PSJ*, **3**, 213
 Feng Y. K., Robinson T. D., Fortney J. J., Lupu R. E., Marley M. S., Lewis N. K., Macintosh B., Line M. R., 2018, *AJ*, **155**, 200
 Feroz F., Hobson M. P., Bridges M., 2009, *MNRAS*, **398**, 1601
 Gillon M., 2018, *Nature Astronomy*, **2**, 344
 Gillon M., et al., 2016, *Nature*, **533**, 221
 Gillon M., et al., 2017, *Nature*, **542**, 456
 Kaltenegger L., Payne R. C., Lin Z., Kasting J., Delrez L., 2022, arXiv e-prints, p. [arXiv:2209.03105](https://arxiv.org/abs/2209.03105)
 Kasting J. F., Whitmire D. P., Reynolds R. T., 1993, *Icarus*, **101**, 108
 Kopparapu R. K., et al., 2013, *ApJ*, **765**, 131

- Kopparapu R. k., Wolf E. T., Arney G., Batalha N. E., Haqq-Misra J., Grimm S. L., Heng K., 2017, *ApJ*, **845**, 5
- Lin Z., MacDonald R. J., Kaltenegger L., Wilson D. J., 2021, *MNRAS*, **505**, 3562
- Lustig-Yaeger J., et al., 2023, *arXiv e-prints*, p. [arXiv:2301.04191](#)
- MacDonald R. J., 2023, *The Journal of Open Source Software*, **8**, 4873
- MacDonald R. J., Lewis N. K., 2022, *ApJ*, **929**, 20
- MacDonald R. J., Madhusudhan N., 2017, *MNRAS*, **469**, 1979
- Rackham B. V., Apai D., Giampapa M. S., 2018, *ApJ*, **853**, 122
- Sebastian D., et al., 2021, *A&A*, **645**, A100
- The JWST Transiting Exoplanet Community Early Release Science Team et al., 2022, *arXiv e-prints*, p. [arXiv:2208.11692](#)
- Trotta R., 2017, *arXiv e-prints*, p. [arXiv:1701.01467](#)
- Turbet M., Bolmont E., Bourrier V., Demory B.-O., Leconte J., Owen J., Wolf E. T., 2020, *Space Sci. Rev.*, **216**, 100
- Turbet M., Bolmont E., Chaverot G., Ehrenreich D., Leconte J., Marcq E., 2021, *Nature*, **598**, 276
- Wakeford H. R., et al., 2019, *AJ*, **157**, 11
- Zhang Z., Zhou Y., Rackham B. V., Apai D., 2018, *AJ*, **156**, 178

This paper has been typeset from a $\text{\TeX}/\text{\LaTeX}$ file prepared by the author.